catalysts

MDPI

Article

# $CO_2$ Reduction Performance with Double-Layered Cu/$TiO_2$ and $P_4O_{10}$/$TiO_2$ as Photocatalysts under Different Light Illumination Conditions

**Akira Nishimura [1,*], Hiroki Senoue [1], Homare Mae [1], Ryo Hanyu [1] and Eric Hu [2]**

[1] Division of Mechanical Engineering, Graduate School of Engineering, Mie University, 1577 Kurimamachiya-cho, Tsu 514-8507, Mie, Japan; 420147@m.mie-u.ac.jp (H.S.); 422m146@m.mie-u.ac.jp (H.M.); 423m139@m.mie-u.ac.jp (R.H.)

[2] School of Electrical and Mechanical Engineering, The University of Adelaide, Adelaide 5005, Australia; eric.hu@adelaide.edu.au

* Correspondence: nisimura@mach.mie-u.ac.jp; Tel.: +81-59-231-9747

**Abstract:** This paper presents an experimental study of using a double-layered Cu/$TiO_2$ and $P_4O_{10}$/$TiO_2$ as photocatalysts for $CO_2$ reduction with an extended wavelength of range light from ultraviolet light (UV) to infrared light (IR). The lights studied were UV + visible light (VIS) + IR, VIS + IR and IR only. This study also investigated the impact of the molar ratio of $CO_2$:$H_2O$ on the $CO_2$ reduction performance. This study revealed that the optimum molar ratio of $CO_2$:$H_2O$ to produce CO was 1:1, irrespective of light illumination condition, which matched the theoretical molar ratio to produce CO according to the reaction scheme of $CO_2$ reduction with $H_2O$. Comparing the results of double-layered Cu/$TiO_2$ and $P_4O_{10}$/$TiO_2$ with those of double-layered $TiO_2$ obtained under the UV + VIS + IR light illumination condition, the highest concentration of formed CO and the molar quantity of formed CO per unit weight of the photocatalyst increased by 281 ppmV and 0.8 μmol/g, in the case of the molar ratio of $CO_2$:$H_2O$ = 1:1. With IR-only illumination, the highest concentration of formed CO and the molar quantity of CO formed per unit weight of the photocatalyst was 251 ppmV and 4.7 μmol/g, respectively.

**Keywords:** Cu/$TiO_2$ photocatalyst; $P_4O_{10}$/$TiO_2$ photocatalyst; double-layered; $CO_2$ reduction; $CO_2$/$H_2O$

check for updates

**Citation:** Nishimura, A.; Senoue, H.; Mae, H.; Hanyu, R.; Hu, E. $CO_2$ Reduction Performance with Double-Layered Cu/$TiO_2$ and $P_4O_{10}$/$TiO_2$ as Photocatalysts under Different Light Illumination Conditions. *Catalysts* **2024**, *14*, 270. https://doi.org/10.3390/catal14040270

Academic Editor: Detlef W. Bahnemann

Received: 11 March 2024
Revised: 15 April 2024
Accepted: 15 April 2024
Published: 17 April 2024



## 1. Introduction

Global warming is a present problem–challenge currently facing the whole world. Photocatalytic $CO_2$ reduction, if developed as a potential technology, would assist in confronting this challenge. $CO_2$ can be converted, with the help of photocatalysts, from $CO_2$ into fuel, e.g., CO, $CH_4$, $CH_3OH$, etc. [1–3]. This study adopted $TiO_2$ as the photocatalyst. $TiO_2$ is the most widely investigated photocatalyst due to its chemical stability, abundance, low cost, and low toxic characteristics [4]. However, $TiO_2$ has some weak points. $TiO_2$ absorbs ultraviolet light (UV) only, which accounts for only 5% in sunlight [5]. The sunlight reaching the earth consists of UV, visible light (VIS), and infrared light (IR) which account for 5%, 45% and 50%, respectively [5]. This study aimed to develop new modified $TiO_2$ photocatalysts which could absorb the light from UV to IR.

According to previous studies [6–20], many approaches to extend the light absorption of photocatalysts from UV to VIS have been conducted. Metal doping is one of the popular approaches to extend the light absorption of photocatalysts from UV to VIS [6,7]. Though some metals such as Pt [8], Au [9] and Pd [10–12] have been investigated, this study focuses on Cu, which is abundant and has a low cost, so it might be easy to apply to industrial needs. According to the review paper [13], Cu/$TiO_2$ displayed good improvements compared to $TiO_2$. This phenomenon occurs since its estimated band gap is relatively the same compared to $TiO_2$ (3.1 eV), and Cu does not shift the absorption spectrum of $TiO_2$. Other previous

studies have reported the impact of the amount of Cu loaded on $TiO_2$ on the performance of $CO_2$ reduction [14]. The highest production rate of $CH_4$ of 1.284 μmol/(g·h) and that of CO of 9.913 μmol/(g·h) were obtained for the weight amount of Cu of 1 wt% under the condition of $CO_2/H_2O$. When increasing the weight amount of Cu, the performance of photocatalytic $CO_2$ reduction decreased. $Cu_2O/TiO_2$ exhibited a production rate of CO, which is 20 times as large as that of $TiO_2$ under the condition of $CO_2/H_2O$ [15]. $Cu_2O$ also showed the photocatalytic performance by itself [16]. The $C_2H_6$ formation of 10 μmol/g was performed by $Cu_2O$, which worked under the light illumination condition of VIS in the case of $CO_2/H_2O$. The authors' previous studies have reported the development of $Cu/TiO_2$ with a pulse arc plasma method to load a fine Cu particle after preparing $TiO_2$ film coated on a netlike glass disc [17,18]. According to these reports [17], $Cu/TiO_2$ exhibited the $CO_2$ reduction performance under the light illumination condition with VIS. Changing the pulse numbers of the fine Cu particles by 100, 200, and 500, the highest molar quantity of CO per weight of the photocatalyst obtained was 12.0 μmol/g for the pulse number of 200 under the light illumination condition without UV. Though the $CO_2$ reduction performance is promoted with the increase in the loading weight of Cu, it is thought that too much Cu loading covers the surface of the $TiO_2$ film [18,19]. It indicates that $CO_2$ and reductants cannot reach the surface of $TiO_2$ film sufficiently due to the optimum loading of Cu. According to previous studies [20], a Z-scheme heterojunction $Cu_2O$/PCN-250 photocatalyst has been utilized for photocatalytic $CO_2$ reduction with $H_2O$ vapor. The significant reduction in the $Cu^{2+}$ content means that the $Cu^{2+}$ species accept photogenerated electrons for the production of $Cu^+$ during the light irradiation. The Fermi energy level of $Cu_2O$ nanoparticles is higher than that of PCN-250, which can lead to interlaced energy levels between two components, providing the possibility of constructing a Z-type heterojunction. From other previous studies [21], Co-MOF/$Cu_2O$ heterojunction has conducted for photocatalytic $CO_2$ reduction with $H_2O$. The Schottky barrier can prevent the back transfer of injected electrons. Hence, under visible-light irradiation, the excited electrons in the CB of $Cu_2O$ can quickly move to the CB of $C_O$-MOF which is above the Ev ($CO_2$/CO, —0.53 V vs. NHE) by the p-n junction induced electric field. Then, the photoexcited electrons remaining in the CB of Co-oxo clusters in Co-MOF react with the absorbed $CO_2$ molecules to produce $CO_2$, and then the photoinduced holes from the VB of Co-MOF move to $Cu_2O$. According to previous research, to extend the light absorption of the photocatalyst from UV to IR or near IR [22–25], many trials have been reported. $W_{18}O_{49}$/g-$C_3N_4$ composite exhibited the production performance of CO of 45 μmol/g and $CH_4$ of 28 μmol/g under the light illumination condition when the wavelength ranged from 200 nm to 2400 nm [22]. $WS_2/Bi_2S_3$ nanotube exhibited the production performance of $CH_3OH$ of 28 μmol/g and $C_2H_5OH$ of 25 μmol/g under the light illumination condition when the wavelength ranged from 420 nm to 1100 nm [23]. CuInZnS decorated g-$C_3N_4$ exhibited the production performance of CO of 38 μmol/g under the light illumination condition when the wavelength ranged from 200 nm to 1000 nm [24]. Hierarchical $ZnIn_2S_4$ nanorods, prepared using the solvothermal method, exhibited the production performance of CO of 54 μmol/g and $CH_4$ of 9 μmol/g [25]. According to the authors' previous studies [26], $P_4O_{10}/TiO_2$ has been investigated. The largest molar quantity of the CO per unit weight of the photocatalyst for $P_4O_{10}/TiO_2$ film in the case of $CO_2/H_2O$ was 2.36 μmol/g under the light illumination condition with IR, while that in case of $CO_2/NH_3$ was 33.4 μmol/g [26].

This study introduced metal doping to explain the basis for adopting Cu and $P_4O_{10}$ as a dopant for $TiO_2$ in this study. Cu is a promising dopant for expanding the light absorption to VIS since many previous studies have reported its good performance [13–18]. In addition, $P_4O_{10}$ is also a promising dopant to expand the light absorption to IR since previous studies carried out by authors have reported its good performance [26]. However, there is no study to clarify the impact of the combination of the photocatalyst absorbing the light with VIS as well as that with IR. If we could develop a photocatalyst absorbing the light ranging from UV to IR, it could then be able to utilize the sunlight for the photocatalytic $CO_2$

reduction in near future. The aim of this study is to clarify the impact of double-layered photocatalysts consisting of $Cu/TiO_2$ and $P_4O_{10}/TiO_2$ on the $CO_2$ reduction performance under the different light illumination conditions. This study adopts $H_2O$ as a reductant for $CO_2$ reduction. The molar ratio of $CO_2$:$H_2O$ is also changed and the impact on the $CO_2$ reduction performance is investigated. According to previous review papers [6,27], $H_2O$ is adopted generally as a reductant. It is necessary to clarify the optimum molar ratio of $CO_2$:$H_2O$ since $H^+$ is needed for the reduction reaction to enhance the $CO_2$ reduction performance. From past studies [28–30], the reaction scheme of $CO_2$ reduction with $H_2O$ can be explained as follows:

Electron-hole pair generation process

$$TiO_2 + h\nu \rightarrow h^+ + e^- \quad (1)$$

Oxidization reaction process

$$H_2O + h^+ \rightarrow OH + H^+ \quad (2)$$

$$\cdot OH + H_2O + h^+ \rightarrow O_2 + 3H^+ \quad (3)$$

Reduction reaction process

$$CO_2 + 2H^+ + 2e^- \rightarrow CO + H_2O \quad (4)$$

$$CO_2 + 8H^+ + 8e^- \rightarrow CH_4 + 2H_2O \quad (5)$$

This study also compared the $CO_2$ reduction performance of double-layered photocatalysts consisting of $Cu/TiO_2$ and $P_4O_{10}/TiO_2$ with that of double-layered $TiO_2$. The light illumination, with a wavelength ranging from 185 nm to 2000 nm, 401 nm to 2000 nm, and 801 nm to 2000 nm, respectively, is changed. In addition, the molar ratio of $CO_2$:$H_2O$ is changed by 1:0.5, 1:1, 1:2, and 1:4. The pulse number of Cu for preparing $Cu/TiO_2$ was 200, which followed the optimum pulse number decided by the authors' previous study [17]. $P_4O_{10}/TiO_2$ has been prepared by sol-gel and the dip-coating processes following the authors' previous studies [26].

## 2. Results and Discussion

### *2.1. Characterization of $Cu/TiO_2$ and $P_4O_{10}/TiO_2$*

Figure 1 shows SEM and EPMA images of $Cu/TiO_2$, which was coated on a netlike glass disc. The black and white SEM images at 1500 times magnification were used for EPMA analysis. As for the EPMA images, the concentrations of each element in the observation area are indicated by the diverse colors. If the amount of element was large, light colors such as white, pink, and red were shown. On the other hand, if the amount of element was small, dark colors such as black and blue were shown. According to Figure 1, it is seen that $TiO_2$ film has a tooth-like shape, coated on the netlike glass fiber. The reason this was caused was thought to be that the temperature distribution of the $TiO_2$ solution adhered on the netlike glass disc was not even during the firing process due to the different thermal conductivities of Ti and $SiO_2$ at 600 K, which were 19.4 W/(m·K) and 1.82 W/(m·K), respectively [31]. Due to the thermal expansion and shrinkage around the netlike glass fiber, a thermal crack formed within the $TiO_2$ film. As a result, the $TiO_2$ film coated on the netlike glass fiber was tooth-like. As for Cu, it is seen that the nano-sized Cu particles are loaded on $TiO_2$ uniformly, since nano-sized Cu particles are emitted by the pulse arc plasma gun process. The center part of the netlike glass disc, with a diameter of 300 μm, was analyzed by EPMA for the measurement of the amount of loaded Cu within $TiO_2$ film. The ratio of Cu to Ti within $Cu/TiO_2$ was counted as 8.3 wt%.

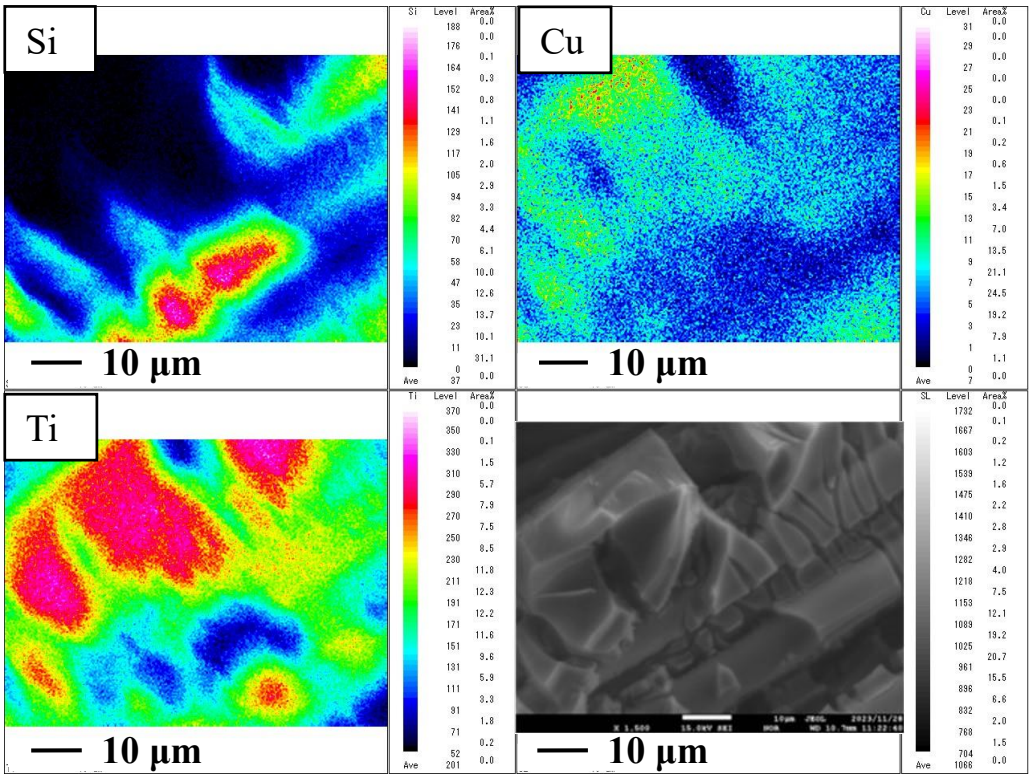


**Figure 1.** SEM and EPMA images of Cu/$TiO_2$ coated on the netlike glass disc, which was prepared in this study.

Figure 2 shows SEM and EPMA images of $P_4O_{10}$/$TiO_2$, which was coated on the netlike glass disc. The black and white SEM images at 1500 times magnification were used for EPMA analysis. According to Figure 2, it can be seen that the $TiO_2$ film had a tooth-like shape coated on the netlike glass fiber as well, which was caused by the same reason explained before for Cu/$TiO_2$. In addition, it can be seen that the nano-sized $P_4O_{10}$ particles were loaded on the $TiO_2$ film. The center part of the netlike glass disc, which had a diameter of 300 µm, was analyzed by EPMA for the amount of loaded Cu within the $TiO_2$ film. The ratio of Cu to Ti within Cu/$TiO_2$ was counted by 6.4 wt%. On the other hand, the total weight of Cu/$TiO_2$ and $P_4O_{10}$/$TiO_2$ was measured by an electron balance which was 0.255 g.

This study has not tested PXRD patterns of prepared photocatalysts, but the crystal type of the $TiO_2$ photocatalyst made was thought to be anatase, since the photocatalyst was prepared at the controlled firing temperature of 623 K. According to the reference presented in [32], the crystal type of the $TiO_2$ photocatalyst would be anatase when prepared below 973 K.

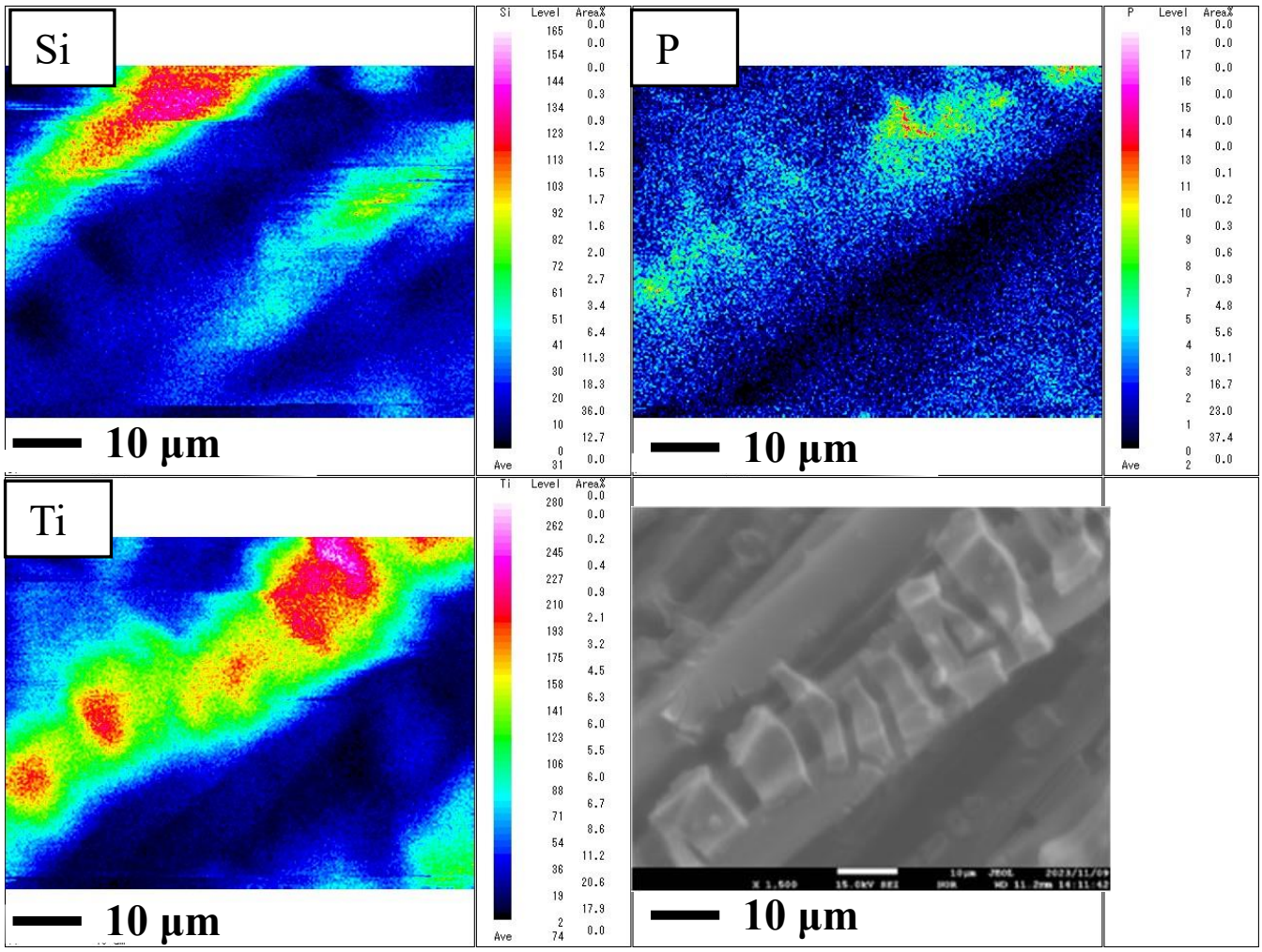


**Figure 2.** SEM and EPMA images of $P_4O_{10}/TiO_2$ coated on the netlike glass disc, which was prepared in this study.

### *2.2. $CO_2$ Reduction Characteristics of Double-Layered $TiO_2$ under the Light Illumination Condition of Xe Lamp with UV + VIS + IR*

Figures 3 and 4 exhibit the change of concentration of formed CO and the molar quantity of CO per unit weight of the photocatalyst with time, respectively. For the expression in the unit of µmol/g in Figure 4, the total weight of $TiO_2$ in double layers was measured by an electron balance, which was 0.136 g. In this study, the $CO_2$ reduction experiment was conducted without the introduction of $H_2O$ and the $CO_2$ reduction experiment under no Xe lamp illumination conditions and the $CO_2$ reduction experiment with $H_2O$ without a photocatalyst were conducted. As a result, no fuel was detected.

Figures 3 and 4 show the highest concentration of formed CO and the molar quantity of CO per unit weight of the photocatalyst of 262 ppmV and 9.5 µmol/g, respectively, which were obtained with the molar ratio of $CO_2$:$H_2O$ = 1:1. This optimal molar ratio agrees with the theoretical molar ratio to produce CO as shown in Equations (1)–(5). The production rate of CO was saturated after 8 h of the illumination from the Xe lamp. The peak of the production rate of CO was observed at 2 h.

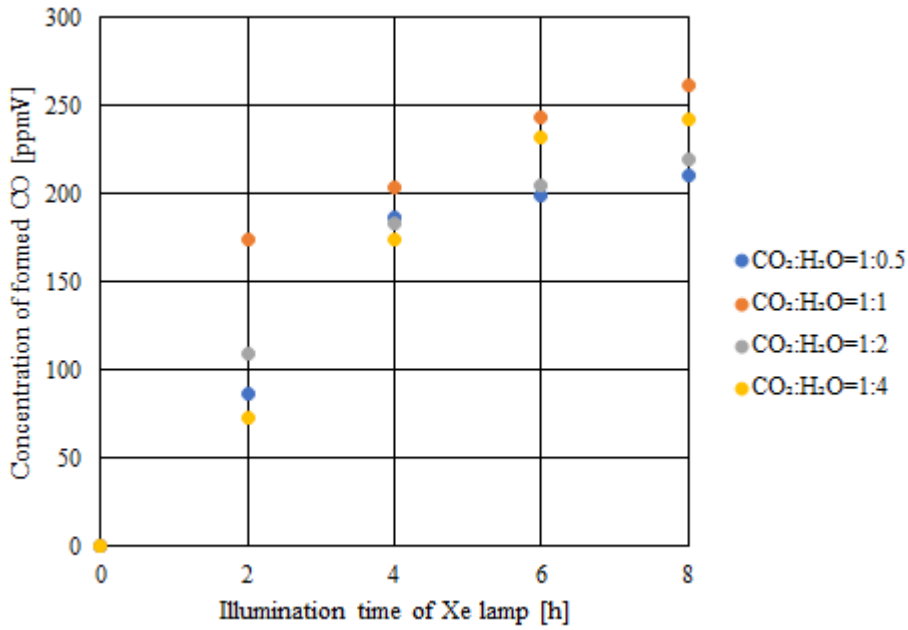


**Figure 3.** Concentration of the formed CO for double-layered $TiO_2$ with UV + VIS + IR illumination.

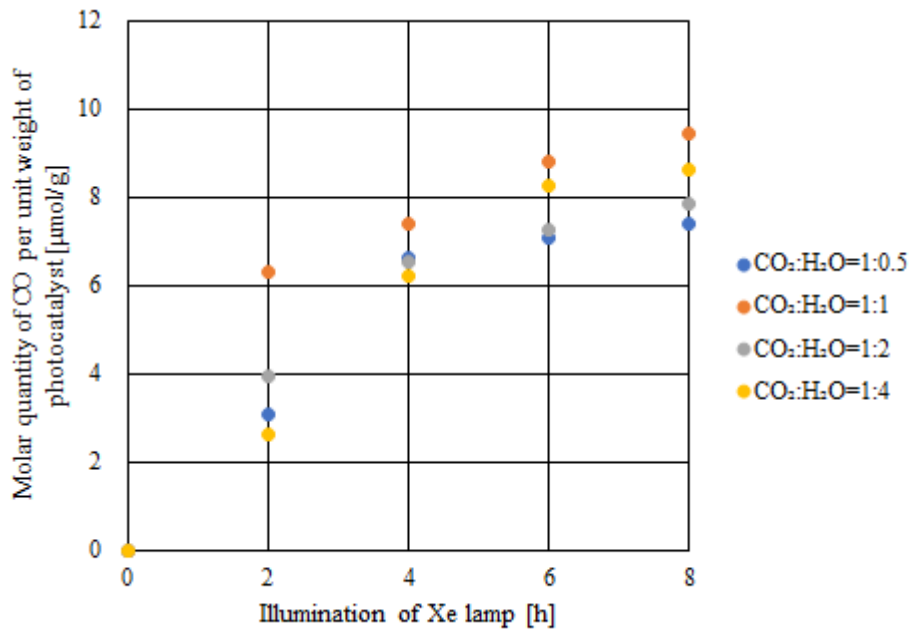


**Figure 4.** Molar quantity of CO per unit weight of the photocatalyst for double-layered $TiO_2$ with UV + VIS + IR illumination.

### *2.3. $CO_2$ Reduction Characteristics of Double-Layered Cu/$TiO_2$ and $P_4O_{10}$/$TiO_2$ with the Illumination of UV + VIS + IR*

Figure 5 illustrates the double-layered Cu/$TiO_2$ and $P_4O_{10}$/$TiO_2$, which also shows the image of double-layered $TiO_2$ for readers to better understand the experimental condition. Figures 6 and 7 show the concentration change of formed CO and the molar quantity of CO per unit weight of the photocatalyst with time, respectively. The data obtained under the light illumination condition with UV + VIS + IR are shown in these figures. In Figure 7, the total weight of double-layered Cu/$TiO_2$ and $P_4O_{10}$/$TiO_2$ was measured by an electron balance, which was 0.255 g. In this study, the $CO_2$ reduction experiment without the introduction of $H_2O$, the $CO_2$ reduction experiment under no Xe lamp illumination

condition, and the $CO_2$ reduction experiment with $H_2O$ without a photocatalyst were conducted. As a result, no fuel was detected.

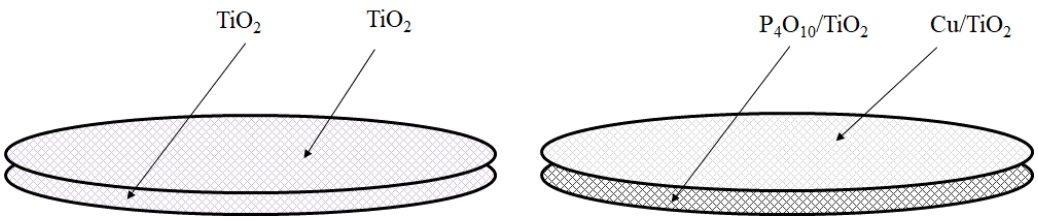


**Figure 5.** Schematic drawing of double-layered photocatalysts.

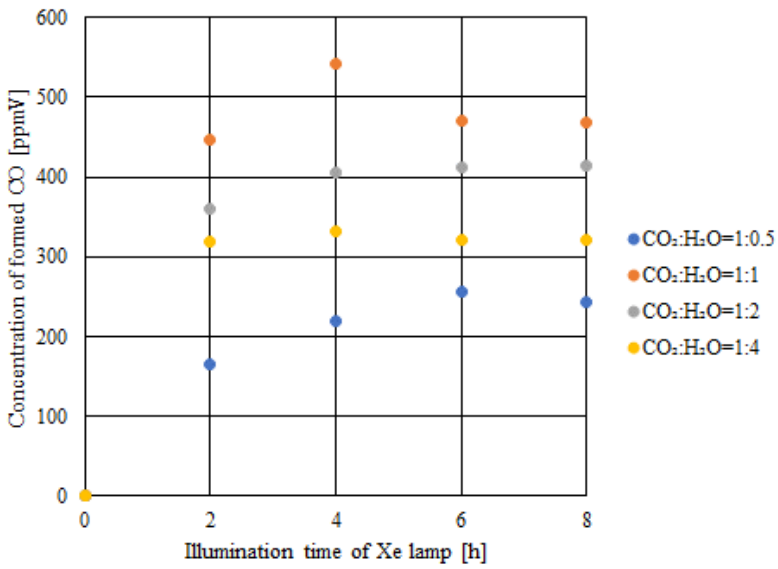


**Figure 6.** Concentration of the formed CO for double-layered $Cu/TiO_2$ and $P_4O_{10}/TiO_2$ with UV + VIS + IR illumination.

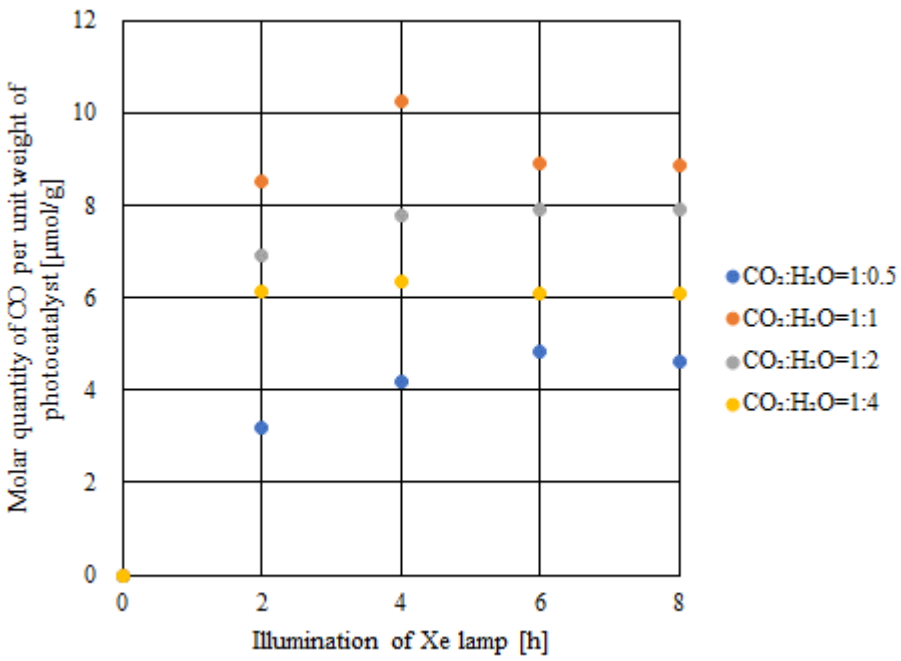


**Figure 7.** Molar quantity of CO per unit weight of the photocatalyst for double-layered $Cu/TiO_2$ and $P_4O_{10}/TiO_2$ with UV + VIS + IR illumination.

According to Figures 6 and 7, the highest concentration of formed CO and the molar quantity of CO per unit weight of the photocatalyst were obtained in the case of the molar ratio of $CO_2$:$H_2O$ = 1:1. The highest concentration of formed CO and the molar quantity of CO per unit weight of the photocatalyst is 543 ppmV and 10.3 μmol/g, respectively. Compared to the results of double-layered $TiO_2$ shown in Figures 3 and 4, the highest concentration of formed CO and the molar quantity of CO per unit weight of the photocatalyst increased by 281 ppmV and 0.8 μmol/g, respectively, with the optimal molar ratio of $CO_2$:$H_2O$ = 1:1. Due to the improvement of light absorption performance with the aid of loading Cu and $P_4O_{10}$, it is thought that the highest concentration of formed CO and the molar quantity of CO per unit weight of the photocatalyst increased, respectively. Since Cu/$TiO_2$ was coated on both surfaces of the netlike glass disc, it is thought that the electron emitted from Cu/$TiO_2$ could reach $P_4O_{10}$/$TiO_2$, which was located under Cu/$TiO_2$. Additionally, it is thought that the balance of electrons and $H^+$, which clarifies the optimum molar ratio according to the reaction scheme as shown in Equations (1)–(5), was not influenced by loading Cu and $P_4O_{10}$ on $TiO_2$ in this study. Therefore, the optimum molar ratio using double-layered Cu/$TiO_2$ and $P_4O_{10}$/$TiO_2$ with UV + VIS + IR illumination in this study follows the theoretical molar ratio to produce CO as shown in Equations (1)–(5).

### *2.4. $CO_2$ Reduction Characteristics of Double-Layered Cu/$TiO_2$ and $P_4O_{10}$/$TiO_2$ with VIS + IR Illumination*

Figures 8 and 9 show the concentration change of formed CO and the molar quantity of CO per unit weight of the photocatalyst with VIS + IR illumination along time, respectively. The total weight of double-layered Cu/$TiO_2$ and $P_4O_{10}$/$TiO_2$ was measured by an electron balance before the experiment, which was 0.255 g.

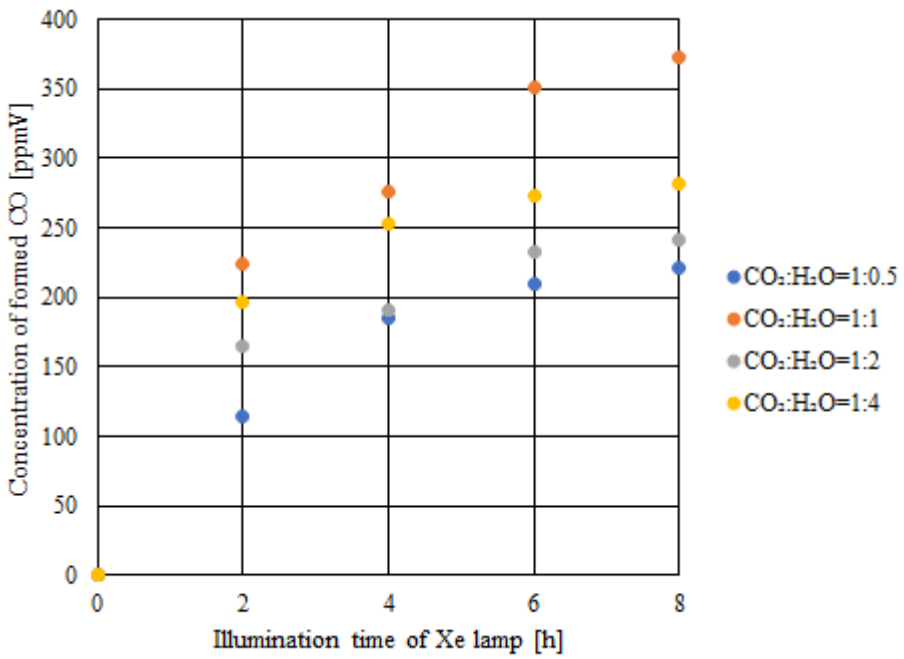


**Figure 8.** Concentration of the formed CO for double-layered Cu/$TiO_2$ and $P_4O_{10}$/$TiO_2$ with VIS + IR illumination.

According to Figures 8 and 9, the highest concentration of formed CO and the molar quantity of CO per unit weight of the photocatalyst are obtained with the molar ratio of $CO_2$:$H_2O$ = 1:1. The highest concentration of formed CO and the molar quantity of CO per unit weight of the photocatalyst was 373 ppmV and 7.1 μmol/g, respectively, as shown in Figures 8 and 9. There was no CO found in the reference experiment conducted, which was with the double-layered $TiO_2$ and VIS + IR. Therefore, loading Cu and $P_4O_{10}$ on $TiO_2$

indeed provided the photocatalyst the absorption capability of VIS + IR. In addition, it also revealed that the optimum molar ratio with double-layered $Cu/TiO_2$ and $P_4O_{10}/TiO_2$ and VIS + IR followed the theoretical molar ratio to produce CO as shown in Equations (1)–(5).

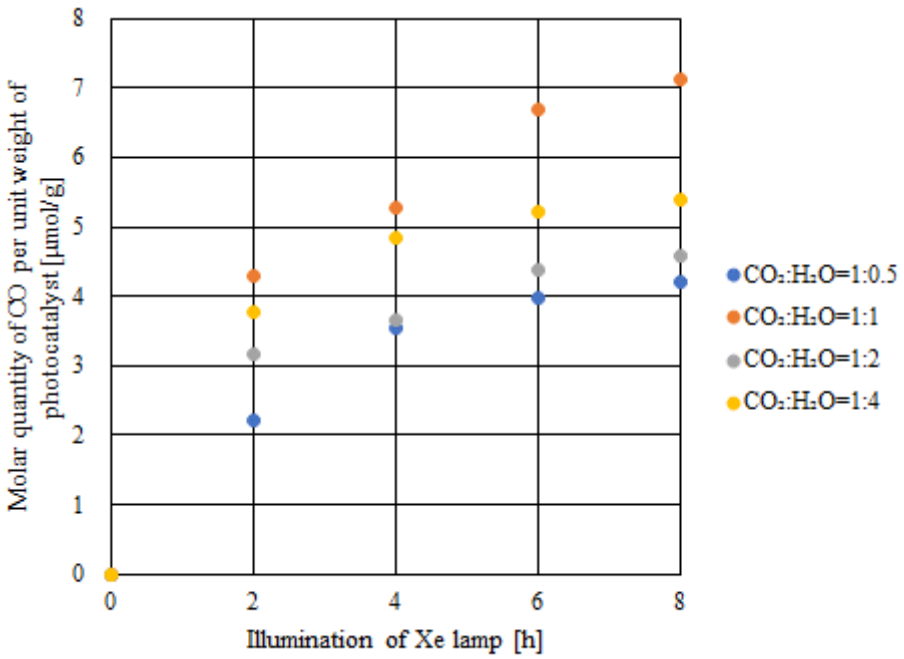


**Figure 9.** Molar quantity of CO per unit weight of the photocatalyst for double-layered $Cu/TiO_2$ and $P_4O_{10}/TiO_2$ with VIS + IR illumination.

In the reference presented in [33], $Cu/TiO_2$ was prepared by the impregnation with aqueous solution of copper acetate, followed by reduction with sodium borohydride. The preparation procedure might influence the chemical/electrochemical state of Cu, which decided the absorption spectrum of $TiO_2$ and the spectrum of $TiO_2$ action in the oxidization reaction. Since this preparation procedure was based on a chemical reaction, it is different from the pulse arc plasma gun method adopted in this study. The pulse arc plasma gun method loads Cu fine particles on the surface of $TiO_2$ physically. Therefore, the role/state played by Cu to $TiO_2$ was different from that in the reference presented in [33].

### *2.5. $CO_2$ Reduction Characteristics of Double-Layered $Cu/TiO_2$ and $P_4O_{10}/TiO_2$ with IR Only Illumination*

Figures 10 and 11 show the concentration of formed CO and the molar quantity of CO per unit weight of the photocatalyst with IR only illumination with time, respectively. The total weight of double-layered $Cu/TiO_2$ and $P_4O_{10}/TiO_2$ was measured by an electron balance, which was 0.255 g.

According to Figures 10 and 11, the highest concentration of formed CO and the molar quantity of CO per unit weight of the photocatalyst were obtained when $CO_2$:$H_2O$ = 1:1. The highest concentration of formed CO and the molar quantity of CO per unit weight of the photocatalyst was 251 ppmV and 4.7 μmol/g, respectively. There was no CO found in the reference experiment conducted, which was with the double-layered $TiO_2$ and IR illumination. Therefore, the $CO_2$ reduction reaction could occur with IR only illumination by loading Cu and $P_4O_{10}$ into the $TiO_2$. In addition, the optimal molar ratio between $CO_2$ and $H_2O$ was also 1:1 for the reaction with IR only, which is the same as with UV + VIS + IR and that with VIS + IR.

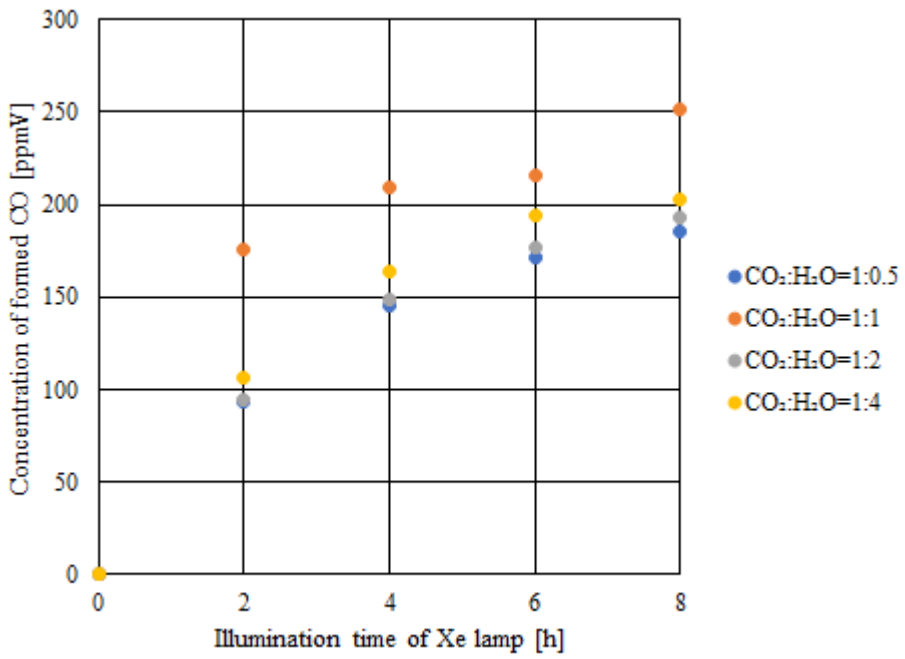


**Figure 10.** Concentration of the formed CO for double-layered $Cu/TiO_2$ and $P_4O_{10}/TiO_2$ with IR only illumination.

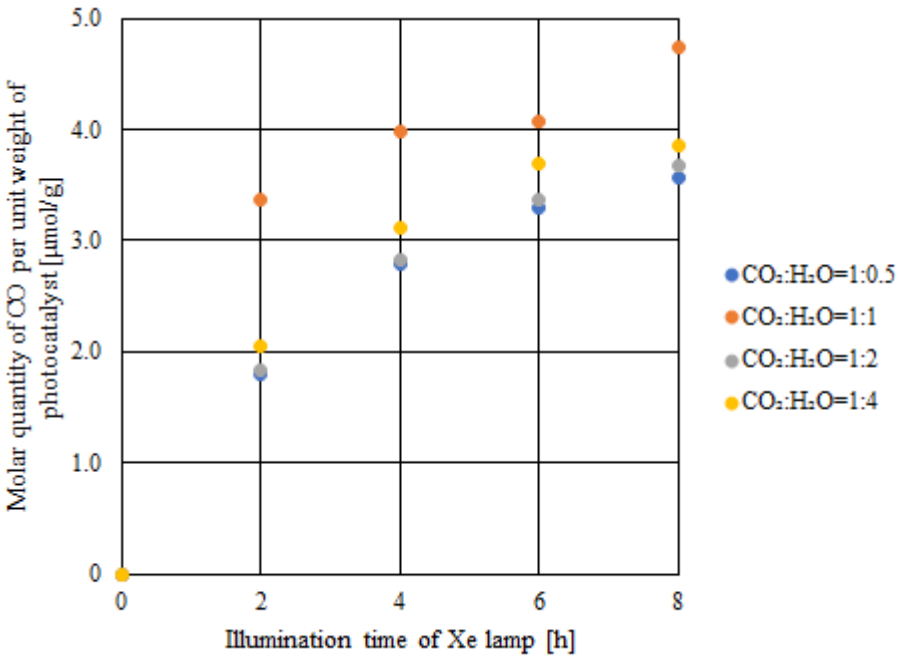


**Figure 11.** Molar quantity of CO per unit of the photocatalyst for double-layered $Cu/TiO_2$ and $P_4O_{10}/TiO_2$ with IR only illumination.

When compared to previous studies [22–26], the $CO_2$ reduction performance with IR only illumination obtained in this study was not high. However, the concept was thought-provoking, i.e., by doping Cu and $P_4O_{10}$ the wavelength of illumination required by $CO_2$ reduction reaction could be extended to IR range.

## 3. Experimental Procedure

### *3.1. Preparation Procedure of $Cu/TiO_2$ and $P_4O_{10}/TiO_2$*

The $TiO_2$ film was prepared by sol-gel and dip-coating processes [34]. $[(CH_3)_2CHO]_4Ti$ (purity of 95 wt%, Nacalai Tesque Co., Ltd., Kyoto, Japan) of 0.3 mol, anhydrous $C_2H_5OH$

(purity of 99.5 wt%, Nacalai Tesque Co., Ltd.) of 2.4 mol, distilled water of 0.3 mol, and HCl (purity of 35 wt%, Nacalai Tesque Co., Ltd.) of 0.07 mol were mixed to prepare $TiO_2$ sol solution. The $TiO_2$ film was coated on netlike glass fiber (SILIGLASS U, Nihonmuki Co., Ltd., Yuki City, Japan) by means of sol-gel and dip-coating processes. The glass fiber, with a diameter of approximately 10 μm, weaved as a net, was collected to be at a diameter of about 1 mm. The porous diameter of the glass fiber and the specific surface area is approximately 1 nm and 400 $m^2/g$, respectively, from the specification of the netlike glass fiber. The netlike glass fiber was composed of $SiO_2$, whose purity was 96 wt%. The opening space of the net glass is approximately 2 mm × 2 mm. The netlike glass fiber with the porous characteristics could capture $TiO_2$ film easily during the sol-gel and dip-coating processes. In addition, $CO_2$ was also more easily absorbed by the prepared photocatalyst due to the porous characteristics. In this study, the netlike glass fiber was cut to be a disc shape with a diameter and the thickness of 50 mm and 1 mm, respectively. The netlike glass disc was dipped into the $TiO_2$ sol solution at the speed of 1.5 mm/s and pulled up it at the fixed speed of 0.22 mm/s. After that, the disc was dried out and fired under the controlled firing temperature (*FT*) and firing duration time (*FD*) to coat $TiO_2$ film on the base material. The *FT* and *FD* was 623 K and 180 s, respectively, in this study.

After the coating of $TiO_2$, Cu was loaded on $TiO_2$ using a pulse arc plasma gun [34], which emitted nano-sized Cu fine particles uniformly with an applied high voltage potential difference of 200 V. Cu fine particles were loaded on both surfaces of $TiO_2$. The pulse number applied could control the quantity of metal loaded on $TiO_2$. This study set the pulse number at 200. This study used the pulse arc plasma gun device (ULVAC, Inc., Chigasaki City, Japan, ARL-300), which had a Cu electrode with a diameter of 10 mm. By setting the distance between the Cu electrode and $TiO_2$ film at 150 mm, Cu particles could be uniformly speared over the $TiO_2$ film. Figure 12 shows the photo of the final coated $Cu/TiO_2$ sample.

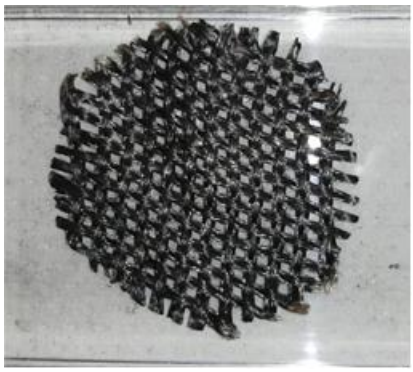

**Figure 12.** Photo of $Cu/TiO_2$ coated on the netlike glass disc.

As to $P_4O_{10}/TiO_2$, $P_4O_{10}$ was made from red P by means of mechanical synthesis [34]. The red P, which had an average diameter of 75 μm (Nacalai Tesque) was filled in a ball mill crusher (AV-1, Asahi Rika Factory, Suginami City, Japan) with $Al_2O_3$ balls. The diameter of the $Al_2O_3$ balls was 3/8 inches (HD-10, NIKKATO COPORATION, Tokyo, Japan). The weight ratio of $Al_2O_3$ balls to red P particles in the ball mill crusher was set at 20 [34]. The rotation speed of 600 rpm was kept for 12 h, and $P_4O_{10}$ was identified to be one type of oxidized P by XPS (PHI Quantera SXM, ULVAC PHI Inc., Chigasaki City, Japan) [26]. The prepared $P_4O_{10}$ particles were put into the $TiO_2$ sol solution and were mixed with the $TiO_2$ sol solution by a magnetic stirrer for 60 min. After that, the netlike glass disc was immersed into this mixed solution. The following dipping and pulling process was the same as explained above. Figure 13 shows the photo of $P_4O_{10}/TiO_2$ coated on the netlike glass disc.


**Figure 13.** Photo of $P_4O_{10}/TiO_2$ coated on the netlike glass disc.

### *3.2. The Characterization Procedure of $Cu/TiO_2$ and $P_4O_{10}/TiO_2$*

The characteristics of the external and crystal structure of $Cu/TiO_2$ and $P_4O_{10}/TiO_2$ film prepared above were evaluated by SEM (JXA-8530F, JEOL Ltd., Akishima City, Japan) and EPMA (JXA-8530F, JEOL Ltd.) [35]. Since the netlike glass disc adopted for base material to coat $Cu/TiO_2$ and $P_4O_{10}/TiO_2$ cannot conduct electricity, the vaporized carbon was deposited by the carbon deposition device (JEE-420, JEOL Ltd.) on the surface of $Cu/TiO_2$ and $P_4O_{10}/TiO_2$ before analyzing the characterization. The thickness of the deposited carbon was about 2030 nm. The acceleration voltage and the current were set at 15 kV and $3.0 \times 10^{-8}$ A, respectively, in order to analyze the external structure.

### *3.3. The Experimental Procedure of $CO_2$ Reduction*

Figure 14 illustrates the experimental apparatus, which is as follows: the reactor, composed of a stainless tube of 100 mm (*H.*) × 50 mm (*I.D.*); $Cu/TiO_2$, which is located over the $P_4O_{10}/TiO_2$, coated on a netlike glass disc of 50 mm (*D.*) × 1mm (*t.*) positioned on the Teflon cylinder of 84 mm (*D.*) × 10 mm (*t.*); a sharp cut filter removing the wavelength of light which is below 400 nm (SCF-49.5C-42L, SIGMA KOKI Co., Ltd., Tokyo, Japan); a 150W Xe lamp (L2175, Hamamatsu Photonics K. K., Hamamatsu City, Japan); mass flow controller; and $CO_2$ gas cylinder (purity of 99.995 vol%) [34]. The size of the reactor chamber is $1.25 \times 10^{-4}$ $m^3$. The light of Xe lamp positioned on the stainless tube illuminates toward $Cu/TiO_2$ and $P_4O_{10}/TiO_2$ passing the sharp cut filter and the quartz glass disc located on the top of the stainless tube. The wavelength of the Xe lamp light ranges from 185 nm to 2000 nm. The sharp cut filter can eliminate UV from the Xe lamp light, resulting in the wavelength of light after the filter ranging from 401 nm to 2000 nm or from 801 nm to 2000 nm. Figure 15 exhibits the light transmittance characteristics after the sharp cut filter to demonstrate, as an example, the removal of the wavelength of light under 400 nm [34]. Though this study has not taken the data on the absorption of light by synthesized catalyst samples, this study exhibits the light transmittance data of the sharp cut filter cutting the wavelength below 400 nm as shown in Figure 15, supporting the UV light illumination condition without UV, i.e., VIS + IR. The authors think this could be evidence for the light absorption range of prepared photocatalysts.

The mean light intensity of light from the Xe lamp without the cut filter was 72.0 $mW/cm^2$ in the wavelength ranging from 185 nm to 2000 nm, while that with the filter was 60.4 $mW/cm^2$ for the wavelength between 401 nm and 2000 nm. Additionally, the mean light intensity of light was 51.2 $mW/cm^2$ in the wavelength ranging from 801 nm to 2000 nm with the sharp cut filter. The light intensities above were measured by the light intensity meter located 55 mm away from the lamp, which was the distance between the Xe lamp and the prepared photocatalyst during the $CO_2$ reduction experiment. Unfortunately, it was impossible to measure the reflect radiation from the walls of reactor by this light intensity meter during the

experiment. The light intensity spectrum data of the Xe lamp used in this study, according to the brochure of Hamamatsu Photonics Corp. [36], is shown in Figure 16.

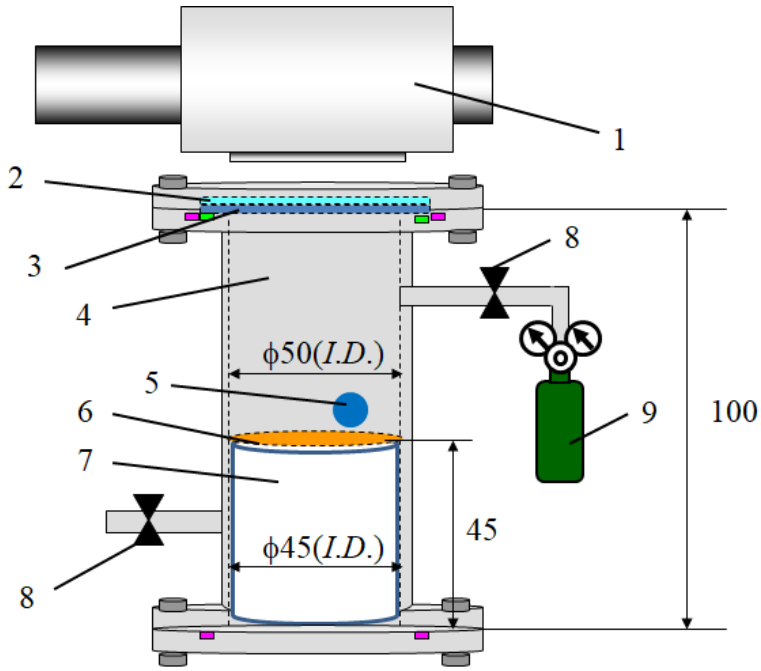


1. Xe lamp, 2. Sharp cut filter, 3. Quartz glass disc, 4. Stainless tube, 5. Gas sampling tap, 6. Photocatalyst, 7. Teflon cylinder, 8. Valve, 9. $CO_2$ gas cylinder (99.995 vol%)

**Figure 14.** Schematic drawing of the $CO_2$ reduction experimental set-up.

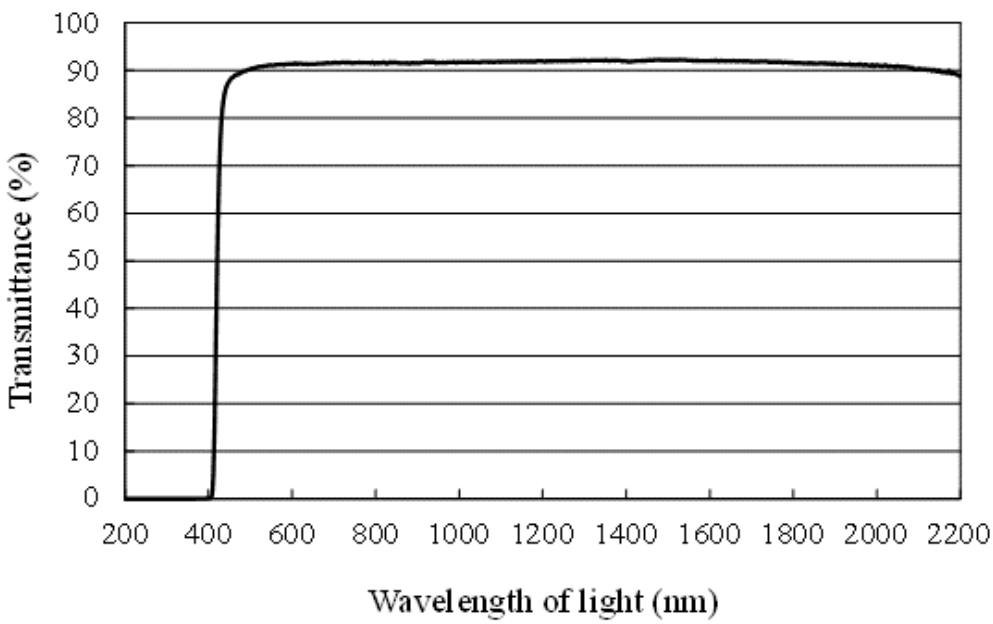


**Figure 15.** Light transmittance data of the sharp cut filter.

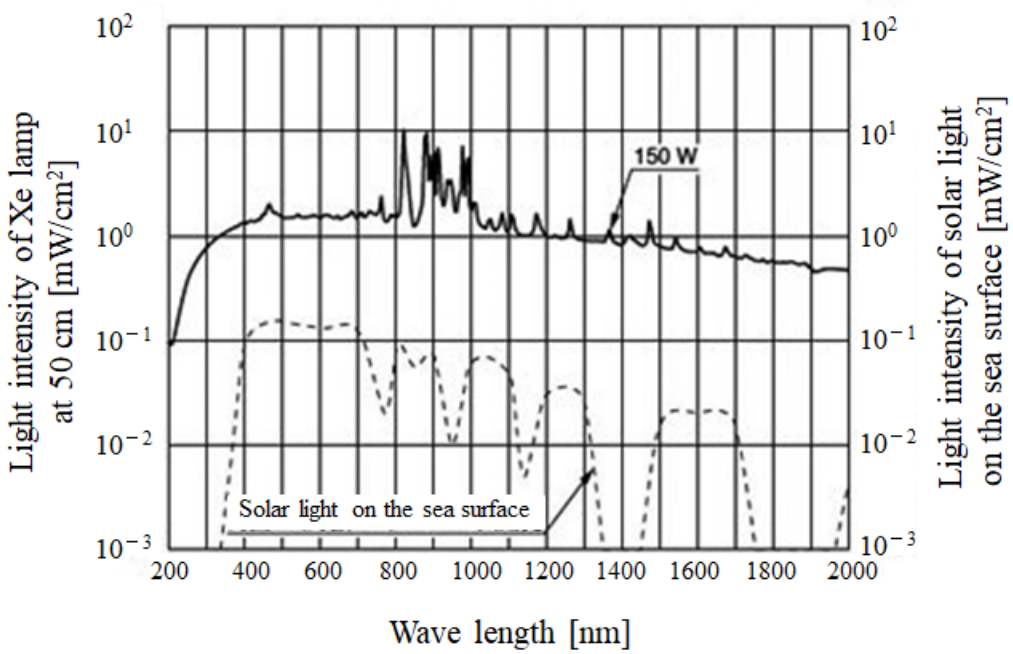


**Figure 16.** Light intensity spectrum data of the Xe lamp used in this study [36].

$CO_2$ gas with the purity of 99.995 vol% was filled in the vacuumed reactor chamber. After that, the valves installed at the inlet and the outlet of reactor were closed during the experiment. The pressure was 0.1 MPa and the gas temperature was set at 298 K in the reactor. Liquid $H_2O$ was injected into the reactor via the gas sampling tap and the Xe lamp was tuned on at the same time. The amount of injected $H_2O$ was changed following the set molar ratio of $CO_2$:$H_2O$. The injected $H_2O$ was vaporized because of the heat of the infrared light components illuminated by the Xe lamp. The temperature in the reactor attained 343 K within an hour, and it was kept at 343 K during the experiment. The molar ratio of $CO_2$:$H_2O$ was changed by 1:0.5, 1:1, 1:2 and 1:4. The reacted gas filled in the reactor was extracted busing a gas syringe via gas sampling tap and it was analyzed by an FID gas chromatograph (GC353B, GL Science, Tokyo, Japan) and a methanizer (MT221, GL Science). The minimum resolution of the FID gas chromatograph and methanizer is 1 ppmV. Regarding the recyclability of photocatalysts, the experiment was conducted three times for the double-layered Cu/$TiO_2$ and $P_4O_{10}$/$TiO_2$ in this study.

## 4. Conclusions

The impact of double-layered photocatalysts consisting of Cu/$TiO_2$ and $P_4O_{10}$/$TiO_2$ on the $CO_2$ reduction performance under different light illumination conditions was studied in this paper. The impact of the molar ratio of $CO_2$:$H_2O$ on the $CO_2$ reduction performance was also investigated. As a result, the following conclusions were drawn:

(i) The highest concentration of formed CO and the molar quantity of CO per unit weight of the photocatalyst were achieved when the molar ratio of $CO_2$:$H_2O$ = 1:1, which matched the theoretical molar ratio to produce CO according to the reaction scheme of $CO_2$ reduction with $H_2O$, irrespective of the light illumination conditions.

(ii) Comparing the results of double-layered Cu/$TiO_2$ and $P_4O_{10}$/$TiO_2$ with the results of double-layered $TiO_2$ obtained under the UV + VIS + IR illumination, the highest concentration of formed CO and the molar quantity of CO per unit weight of the photocatalyst increased by 281 ppmV and 0.8 μmol/g, respectively, when $CO_2$:$H_2O$ = 1:1.

(iii) With VIS + IR illumination, the highest concentration of formed CO and the molar quantity of CO per unit weight of the photocatalyst reached 373 ppmV and 7.1 μmol/g, respectively. This proves that $CO_2$ reduction could be activated with VIS + IR illumination if $TiO_2$ loaded with Cu and $P_4O_{10}$ was used as the photocatalyst.

(iv) With only IR illumination, the highest concentration of formed CO and the molar quantity of CO per unit weight of the photocatalyst was 251 ppmV and 4.7 μmol/g, respectively. This proves that $CO_2$ reduction reaction could be activated with IR only illumination if $TiO_2$ loaded with Cu and $P_4O_{10}$ was used as the photocatalyst.

**Author Contributions:** Conceptualization and writing—original draft preparation, A.N.; data curation, H.S.; methodology, H.M. and R.H.; writing—review and editing, E.H. All authors have read and agreed to the published version of the manuscript.

**Funding:** This research was funded by Mie University and JSPS KAKENHI Grant Number JP21K04769.

**Data Availability Statement:** The data presented in this study are available.

**Conflicts of Interest:** The authors declare no conflicts of interest.

## References

1. Jesic, D.; Jurkovic, L.D.; Pohar, A.; Suhadolnik, L.; Likozar, B. Engineering Photocatalytic and Photoelectrocatalytic $CO_2$ Reduction Reactions: Mechanisms, Intrinsic Kinetics, Mass Transfer Resistances, Reactors and Multi-scale Modeling Simulations. *Chem. Eng. J.* **2021**, *407*, 126799. [CrossRef]
2. Kaushik, R.; Singh, P.K.; Halder, A. Modulation Strategies in Titania Photocatalyst for Energy Recovery and Environmental Remediation. *Catal. Today* **2022**, *384–386*, 45–69. [CrossRef]
3. Wang, Z.W.; Shi, Y.Z.; Liu, C.; Kang, Y.Y.; Wu, L. $Cu^+$-$Ti^{3+}$ Interface Interaction Mediated $CO_2$ Coordination model for Controlling the Selectivity of Photocatalytic Reduction $CO_2$. *Appl. Catal. B Environ.* **2022**, *301*, 120803. [CrossRef]
4. Jiang, Z.; Zhang, X.; Yuan, Z.; Chen, J.; Huang, B.; Dionysiou, D.D.; Yang, G. Enhanced Photocatalytic $CO_2$ Reduction via the Synergetic Effect between Ag and Activated Carbon in $TiO_2$/AC-Ag Ternary Composite. *Chem. Eng. J.* **2018**, *348*, 592–598. [CrossRef]
5. Kumar, A.; Kumar, P.; Borker, R.; Bansiwal, A.; Labhsetwar, N.; Jain, S.L. Metal-organic hybrid: Photoreduction of $CO_2$ using graphitic carbon nitride supported heteroleptic iridium complex under visible light irradiation. *Carbon* **2017**, *123*, 371–379. [CrossRef]
6. Nahar, S.; Zain, M.F.M.; Kadhum, A.A.H.; Hasan, F.A.; Hasan, M.R. Advances in Photocatalytic $CO_2$ Reduction with Water: A Review. *Materials* **2017**, *10*, 629. [CrossRef] [PubMed]
7. Ola, O.; Maroto-Valer, M.M. Review of Material Design and Reactor Engineering on $TiO_2$ Photocatalysis for $CO_2$ Reduction. *J. Photochem. Photobiol. C Photochem. Rev.* **2015**, *24*, 16–42. [CrossRef]
8. Tasbihi, M.; Fresno, F.; Simon, U.; Villar-Garcia, I.J.; Perez-Dieste, V.; Escudero, C.; O'Shea, V.A.D.L.P. On the Selectivity of $CO_2$ Photoreduction towards $CH_4$ Using Pt/$TiO_2$ Catalysts Supported on Mesoporous Silica. *Appl. Catal. B Environ.* **2018**, *239*, 68–76. [CrossRef]
9. Remiro-Buenamanana, S.; Garcia, H. Photoassisted $CO_2$ Conversion to Fuels. *ChemCatChem* **2019**, *11*, 342–536. [CrossRef]
10. Yu, Y.; Lan, Z.; Guo, L.; Wang, E.; Yao, J.; Cao, Y. Synergetic Effects of Zn and Pd Species in $TiO_2$ towards Efficient Photo-reduction of $CO_2$ into $CH_4$. *R. Soc. Chem.* **2018**, *42*, 483–488.
11. Singhal, N.; Kumar, U. Noble Metal Modified $TiO_2$: Selective Photoreduction of $CO_2$ to Hydrocarbons. *Mol. Catal.* **2017**, *439*, 91–99. [CrossRef]
12. Yui, T.; Kan, A.; Saitoh, C.; Koike, K.; Ibusuki, T.; Ishitani, O. Photochemical Reduction of $CO_2$ Using $TiO_2$: Effects of Organic Adsorbates on $TiO_2$ and Deposition of Pd onto $TiO_2$. *ACS Appl. Mater. Interfaces* **2011**, *3*, 2594–2600. [CrossRef] [PubMed]
13. Abdulah, H.; Khan, M.M.R.; Ong, H.R.; Yaakob, Z. Modified $TiO_2$ Photocatalyst for $CO_2$ Photocatalytic Reduction: An Overview. *J. $CO_2$ Util.* **2017**, *22*, 15–32. [CrossRef]
14. Camarillo, R.; Toston, S.; Martinez, F.; Jimenez, C.; Rincon, J. Improving the Photo-reduction of $CO_2$ to Fuels with Catalysts Synthesized under High Pressure: Cu/$TiO_2$. *J. Chem. Technol. Biotechnol.* **2018**, *93*, 1237–1248. [CrossRef]
15. Aguirre, M.E.; Zhou, R.; Engene, A.J.; Guzman, M.I.; Grela, M.A. $Cu_2O$/$TiO_2$ Heterostructures for $CO_2$ Reduction through a Direct Z-scheme: Protecting $Cu_2O$ from Photocorrosion. *Appl. Catal. B Environ.* **2017**, *217*, 485–493. [CrossRef]
16. Kulandaivalu, T.; Rashid, S.A.; Sabli, N.; Tan, T.L. Visible Light Assisted Photocatalytic Reduction of $CO_2$ to Ethane Using CQDs/$Cu_2O$ Nanocomposite Photocatalyst. *Diam. Relat. Mater.* **2019**, *91*, 64–73. [CrossRef]
17. Nishimura, A.; Sakakibara, Y.; Koshio, A.; Hu, E. The Impact of Amount of Cu on $CO_2$ Reduction Performance of Cu/$TiO_2$ with $NH_3$ and $H_2O$. *Catalysts* **2021**, *11*, 610. [CrossRef]
18. Zhao, H.; Rao, G.; Wang, L.; Xu, L.; Liu, L.; Li, X. Synthesis of Novel MgAl Layered Double Oxide Grafted $TiO_2$ Cuboids and their Photocatalytic Activity on $CO_2$ Reduction with Water Vapor. *Catal. Sci. Technol.* **2015**, *5*, 3288–3295. [CrossRef]
19. Zhang, R.; Huang, Z.; Li, C.; Zuo, Y.; Zhou, Y. Monolithic g-$C_3N_4$/Reduced Graphene Oxide Aerogel with in Situ Embedding of Pd Nanoparticles for Hydrogeneration of $CO_2$ to $CH_4$. *Appl. Suf. Sci.* **2019**, *475*, 953–960. [CrossRef]
20. Yang, M.M.; Cao, J.M.; Qi, G.D.; Shen, X.Y.; Yan, G.Y.; Wang, Y.; Dong, W.W.; Zhao, J.; Li, D.S.; Zhang, Q. Construction of low-cost z-scheme heterojunction $Cu_2O$/PCN-250 photocatalysts simultaneously for the enhanced photoreduction of $CO_2$ to alcohols and photooxidation of water. *Inorg. Chem.* **2023**, *62*, 15963–15970. [CrossRef]

21. Dong, W.W.; Jia, J.; Wang, Y.; An, J.R.; Yang, O.Y.; Gao, X.J.; Liu, Y.L.; Zhao, J.; Li, D.S. Visible-light-driven solvent-free photocatalytic $CO_2$ reduction to CO by Co-MOF/$Cu_2O$ heterojunction with superior selectivity. *Chem. Eng. J.* **2022**, *438*, 135622. [CrossRef]
22. Hong, L.F.; Guo, R.T.; Yuan, Y.; Ji, X.Y.; Lin, Z.D.; Gu, J.W.; Pan, W.G. Urchinlike $W_{18}O_{49}$/g-$C_3N_4$ Z-Scheme Heterojunction for Highly Efficient Photocatalytic Reduction of $CO_2$ under Full Spectrum Light. *Energy Fuels* **2021**, *35*, 11468–11478. [CrossRef]
23. Dai, W.; Yu, J.; Luo, S.; Hu, X.; Yang, L.; Zhang, S.; Li, B.; Luo, X.; Zou, J. WS2 Quantum Dots Seeding in $Bi_2S_3$ Nanotubes: A Novel Vis-NIR Light Sensitive Photocatalyst with Low-Resistance Junction Interface for $CO_2$ Reduction. *Chem. Eng. J.* **2020**, *389*, 123430. [CrossRef]
24. Gan, J.; Wang, H.; Hu, H.; Su, M.; Chen, F.; Xu, H. Efficient Synthesis of Tunable Band-Gap CuInZnS Decorated g-$C_3N_4$ Hybrids for Enhanced $CO_2$ Photocatalytic Reduction and Near-Infrared- Triggered Photordegradation Performance. *Appl. Surf. Sci.* **2021**, *564*, 150396. [CrossRef]
25. Yu, M.; Lv, X.; Idris, A.M.; Li, S.; Lin, J.; Lin, H.; Wang, J.; Li, Z. Upconversion Nanoparticles Coupled with Hierarchical ZnIn2S4 Nanorods as a Near-Infrared Responsive Photocatalyst for Photocatalytic $CO_2$ Reduction. *J. Colloid Interface Sci.* **2022**, *612*, 782–791. [CrossRef]
26. Nishimura, A.; Mae, H.; Kato, T.; Hu, E. Utilization from ultraviolet to infrared light for $CO_2$ reduction with $P_4O_{10}$/$TiO_2$ photocatalyst. *Phys. Astron. Int. J.* **2022**, *6*, 145–154. [CrossRef]
27. Tahir, M.; Amin, N.S. Advances in Visible Light Responsive Titamium Oxide Based Photocatalysts for $CO_2$ Conversion to Hydrocarbon Fuels. *Energy Convers. Manag.* **2013**, *76*, 194–214. [CrossRef]
28. Goren, Z.; Willner, I.; Nelson, A.J. Selective Photoreduction of $CO_2$/HCO3− to Formate by Aqueous Suspensions and Colloids of Pd-$TiO_2$. *J. Physic. Chem.* **1990**, *94*, 3784–3790. [CrossRef]
29. Tseng, I.H.; Chang, W.C.; Wu, J.C.S. Photoreduction of $CO_2$ Using Sol-gel Derived Titania and Titania-supported Copper Catalysts. *Appl. Catal. B* **2002**, *37*, 37–38. [CrossRef]
30. Izumi, Y. Recent Advances in the Photocatalytic Conversion of Carbon Dioxide to Fuels with Water and/or Hydrogen Using Solar Energy and Beyond. *Coord. Chem. Rev.* **2013**, *257*, 171–186. [CrossRef]
31. Japan Society of Mechanical Engineering. *Heat Transfer Hand Book*, 1st ed.; Maruzen: Tokyo, Japan, 1993; pp. 367–369.
32. Yokoi, Y.; Ando, N.; Yokoi, H.; Iwashita, H.; Suzuki, R. Application of sintered titanium dioxide to biomaterials: Sintering temperature of anatase-type $TiO_2$ and cell proliferation of L929 cells. *J. Jpn. Soc. Oral Implantol.* **2012**, *25*, 262–270. Available online: https://www.jstage.jst.go.jp/article/jsoi/25/2/25_262/_pdf/-char/en (accessed on 14 April 2024).
33. Kovalevskiy, N.S.; Lyulyukin, M.N.; Kozlov, D.V.; Selishchev, D.S. Cu-grafted $TiO_2$ photocatalysts: Effect of Cu on the action spectrum of composite materials. *Mendeleev Commun.* **2021**, *31*, 644–646. [CrossRef]
34. Nishimura, A.; Ishida, N.; Tatematsu, D.; Hirota, M.; Koshio, A.; Kokai, F.; Hu, E. Effect of Fe Loading Condition and Reductants on $CO_2$ Reduction Performance with Fe/$TiO_2$ Photocatalyst. *Int. J. Photoenergy* **2017**, *2017*, 1625274. [CrossRef]
35. Licensable Patent Information Database. P2009-184861A. 2022. Available online: https://plidb.inpit.go.jp (accessed on 14 April 2024).
36. Brochure of Hamamatsu Photonics Corp. 2000. Available online: https://www.hamamatsu.com/content/dam/hamamatsu-photonics/sites/documents/99_SALES_LIBRARY/etd/Xe-HgXe_TLS1016J.pdf (accessed on 14 April 2024).